

**ISO 16063-11:  
PRIMARY VIBRATION CALIBRATION BY LASER INTERFEROMETRY.  
EVALUATION OF SINE APPROXIMATION REALISED BY FFT.**

*Torben R. Licht<sup>1</sup> and Sven Erik Salboel<sup>2</sup>*

<sup>1</sup>DPLA and Brüel & Kjaer S&V, Naerum, Denmark, [trlicht@bksv.com](mailto:trlicht@bksv.com)

<sup>2</sup>DPLA and Brüel & Kjaer S&V, Naerum, Denmark, [sesalbol@bksv.com](mailto:sesalbol@bksv.com)

**Abstract:** Laser interferometry has been used for accelerometer calibration since the late sixties using counters for fringe counting and determination of zeroes at higher frequencies. As the digital techniques evolved during the eighties and nineties it became possible to make more sophisticated treatment of the complex output signals from the interferometer detectors. This was described in the revision of the previous standard ISO 5347-1 resulting in the new ISO 16063-11 in 1999. In this the so-called sine approximation method was introduced. As the input is known to be a sine, a least square fitting of the results calculated from the interferometer output gave good results. The fitting is basically a filtering at the known frequency. Therefore with the advanced high-resolution FFT analysers available today it is logical to use such analysers to do the filtering.

A system has been realised following these ideas. This will be described, and the evaluation of the system's sensitivity to different imperfections, e.g. noise and gain differences in the interferometer output, will be reported. The evaluation is made using computer generated test signals and the technique can also be used to verify the system whenever needed.

**Keywords:** vibration, calibration, interferometry, FFT analysis, accelerometer.

## 1. LASER INTERFEROMETRY

An example of a classical laserinterferometric setup is shown in Figure 1.

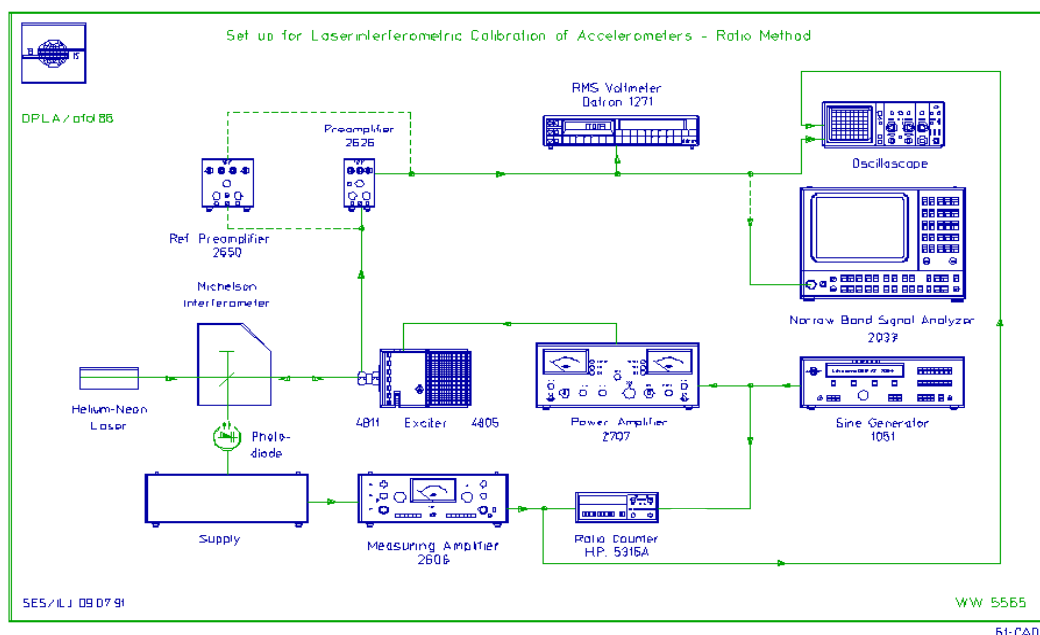


Figure 1. Classic laserinterferometric setup.

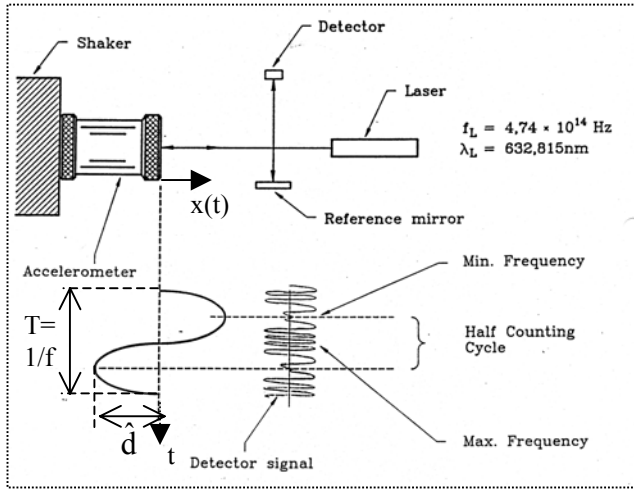


Figure 2. Fringe counting

Figure 2 shows the basic fringe counting or ratio principle and Figure 3 the calculations needed to find the acceleration with an example at  $50 \text{ ms}^{-2}$  and  $159.155 \text{ Hz}$ .

Vibration  $x(t) = \hat{d} \sin(\omega t + \varphi)$

$$R_f = \frac{8\hat{d}}{\lambda} \quad \hat{a} = \hat{d}\omega^2$$

$$R_f = \frac{8\hat{a}}{\omega^2\lambda} = \frac{8\sqrt{2}a_{\text{rms}}}{(2\pi f)^2\lambda}$$

Example:  
 $a_{\text{rms}} = 50 \text{ m/s}^2$  and  $f = 159.155 \text{ Hz}$  ( $\omega = 1000$ )  
 gives  
 $R_f = 893.92$

Figure 3. Fringe formulas

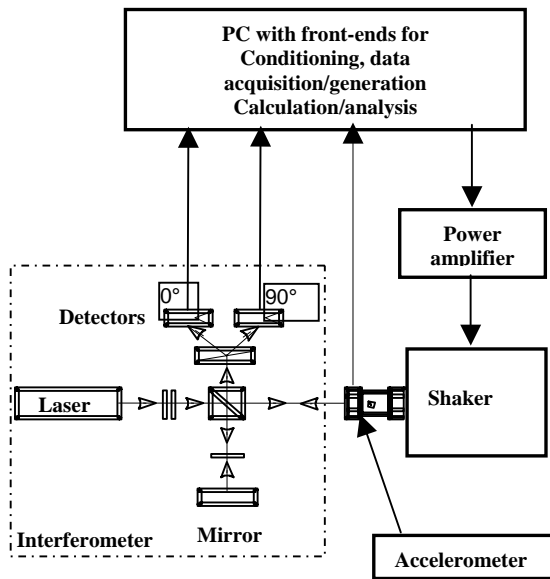


Figure 4. New setup with quadrature output.

Figure 4 shows the principle of more recent systems. The interferometer, which can be an integrated unit or a set-up as shown, provides two outputs in quadrature.

These signals and the signal from the accelerometer are all conditioned by suitable preamplifiers if necessary and then digitized. The output for generation of the vibration through the power amplifier and shaker is also generated digitally and then converted to an analog output signal. The same clock controls all digitizing. The PC is the heart of all these functions and controls the system.

## 2. ISO 16063-11: PRIMARY VIBRATION CALIBRATION BY LASER INTERFEROMETRY

The most commonly used method in systems, as the one sketched in Figure 4 is Method 3, sine approximation as described in [1].

This method results in a discrete time series of modulation phase values calculated from the digitized detector outputs  $u_1(t_i)$  and  $u_2(t_i)$  using the relationship

$$\varphi_{\text{Mod}}(t_i) = \arctan \frac{u_2(t_i)}{u_1(t_i)} + p\pi \quad (1)$$

where the integer  $p$  has to be chosen properly to avoid discontinuities.

These results are then used to create  $N+1$  equations

$$\varphi_{\text{Mod}}(t_i) = A \cos \omega t_i - B \sin \omega t_i + C \quad (2)$$

to be solved using the least squares method to find  $A$ ,  $B$  and  $C$ .

$$i = 0, 1, 2, \dots, N$$

$$A = \hat{\varphi}_M \cos \varphi_s$$

$$B = \hat{\varphi}_M \sin \varphi_s$$

$C$  is a constant

$\omega$  is the angular frequency of vibration  $\omega = 2\pi f$

$\varphi_s$  is the initial phase of the displacement

$N+1$  is the number of samples taken synchronously over the measurement period.

$f$  is the vibration frequency known by the system.

If we look at the Discrete Fourier Transformation (DFT), of any time series of  $N+1$  elements taken over a time  $T = 1/f$  this can be described by

$$\varphi_{\text{Mod-DFT}}(t_i) = C' + \sum_{n=1}^N \hat{\varphi}_{Mn} \cos(n\omega t_i + \varphi'_s) =$$

$$C' + \sum_{n=1}^N \hat{\varphi}_{Mn} (\cos \varphi'_s \cos n\omega t_i - \sin \varphi'_s \sin n\omega t_i) = \dots \quad (3)$$

$$C' + A' \cos \omega t_i - B' \sin \omega t_i$$

$$+ \sum_{n=2}^N \hat{\varphi}_{Mn} (\cos \varphi'_s \cos n\omega t_i - \sin \varphi'_s \sin n\omega t_i)$$

Then the least squares method would require minimizing

$$\sum_{i=1}^N (\varphi_{\text{Mod-DFT}}(t_i) - \varphi_{\text{Mod}}(t_i))^2 = \sum_{i=1}^N \left( \begin{aligned} &C' + A' \cos \omega t_i - B' \sin \omega t_i \\ &+ \sum_{n=2}^N \hat{\varphi}_{Mn} (\cos \varphi'_s \cos n\omega t_i - \sin \varphi'_s \sin n\omega t_i) \\ &-(C + A \cos \omega t_i - B \sin \omega t_i) \end{aligned} \right)^2 \dots\dots\dots(4)$$

If we set

$$\hat{\varphi}_{M1} = \hat{\varphi}_M \quad \text{and} \quad \varphi'_s = \varphi_s$$

i.e.

$$A' = A; \quad B' = B$$

and also  $C' = C$

then we obtain

$$\sum_{i=1}^N (\varphi_{\text{Mod-DFT}}(t_i) - \varphi_{\text{Mod}}(t_i))^2 = \sum_{i=1}^N \left( \sum_{n=2}^N \hat{\varphi}_{Mn} (\cos \varphi_s \cos n\omega t_i - \sin \varphi_s \sin n\omega t_i) \right)^2 = \dots\dots\dots(5)$$

$$\sum_{i=1}^N \left( \sum_{n=2}^N \hat{\varphi}_{Mn} (\cos(n\omega t_i + \varphi_s)) \right)^2$$

Which becomes equal to zero if all  $\hat{\varphi}_{Mn}$  for  $n \geq 2$  are zero. This means basically that only the fundamental frequency is left and all harmonics rejected as one could expect. If  $m$  times longer records are used the vibration frequency will just be the  $m$ 'th harmonic ( $m$  being an integer  $\geq 2$ ).

Thus it is proved that using DFT (or the faster FFT) with appropriate sampling and taking out the values for the proper frequency is identical to the described sine approximation method.

## 2.1 The role of FFT analyzers

Using standard FFT analyzers and selecting vibration frequencies and settings of the analyzer in such a way that the vibration frequency coincides with a center frequency of one of the frequency bands (which is the same as requiring the record length to be a multiple of the period of the vibration frequency) will give exactly the same results as described above (also independent of any time window used).

It is however desirable to permit the free choice of frequencies, and therefore a special flat-top time window can be used in FFT analysis. This requires a somewhat longer time record, but will give the correct parameters for the vibration frequency component within 0.03% for frequencies less than 0.43 times the frequency resolution used for analysis from the center frequency and maximum 0.113% off at the worst point in the middle between two analysis bands. The response of such a filter is shown in Figure 5 where the values for the distance from the frequency to the center frequency of a band is normalized by the frequency resolution  $df$ . The time window in Figure 6.

This means that we can use a high-resolution calibrated analyzer to measure the ratio between the displacement calculated from the laser signals and the accelerometer output, and still get very high accuracy. Even in the worst case, which can be avoided, it will only contribute with 0.1%. A correction is also possible

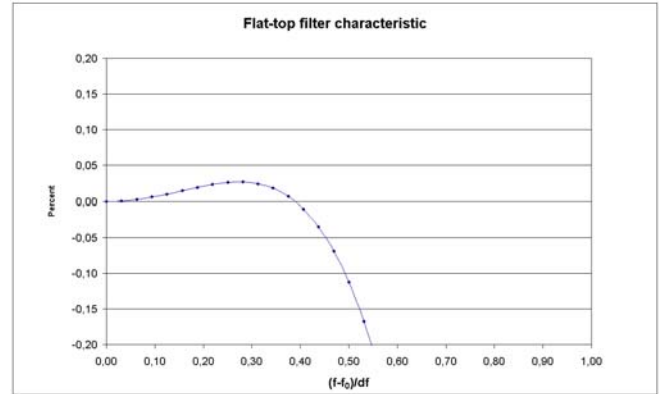


Figure 5. Flat-top filter characteristics.

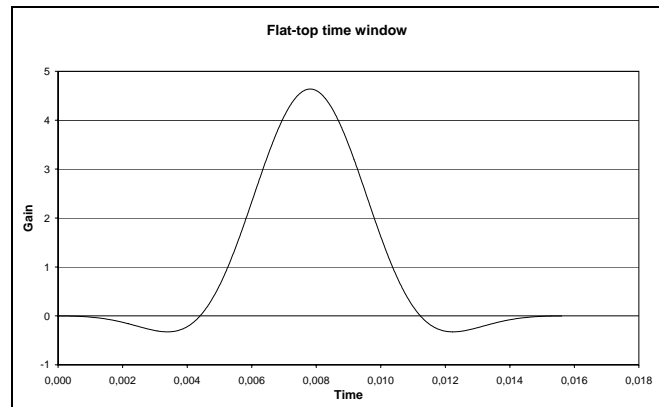


Figure 6. Flat-top time window

The calibration of the analyzer can be performed in different ways. One method that fits well with the procedures in many laboratories is to base it on a high precision digital multi meter (DMM). This can give accuracies in the order of 0.03 to 0.1 % ( $2\sigma$  values) above 10 Hz and about twice these values below 10 Hz. Automating the calibration and storing the results in a database facilitates the automatic correction of the measurements afterwards transferring the DMM accuracies to the analyzer nearly without any increase in uncertainty. Simultaneously it can provide traceability.

The voltmeter used to calibrate the analyzer is in a sampling mode below 2 Hz. This is necessary as the voltmeters are not very accurate for normal AC measurements below 2 Hz.

### 3. EXAMPLE OF IMPLEMENTATION

A system following the ideas outlined above has been implemented. The block diagram in Figure 7 shows the data flow through the system that is based on a Brüel & Kjaer analyzer in the PULSE family.

The initial operation is an A/D conversion (16 bit) and recording of raw data from the two detectors in quadrature and the accelerometer onto the harddisk. Maximum sample rate is used and all channels are sampling synchronously to be sure to keep the phase relationships. Streaming the data directly to the harddisk makes it unimportant how large the files are but naturally large amounts of data take longer time

to process. This permits e.g. measurements at very low frequencies, down to 0.1 Hz giving files of several hundred Megabytes each.

When the recording of data at each of the desired frequencies is finished the data from the laser are processed and stored as UFF files together with the data from the accelerometer. After finishing all frequencies these files ( $x(t)$  and  $a(t)$ ) are then read back sequentially into the PULSE Time Analyzer, i.e. as files, not through any analyzer hardware. Here the FFT analyzer treats the signals and send the result to the calibration software which apply any final corrections (from the DMM data) and sends the result to the harddisk and the display.

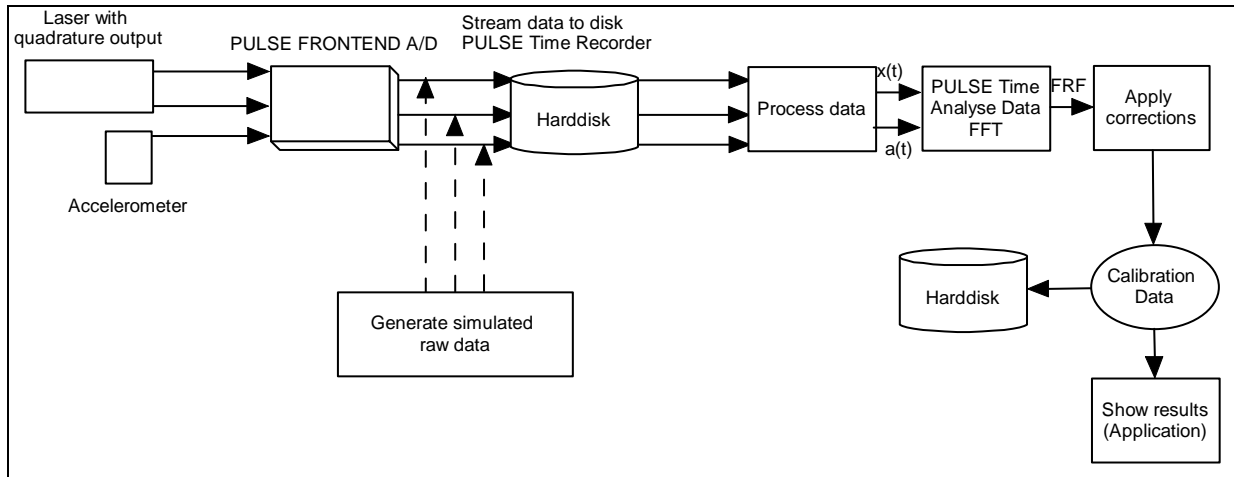


Figure 7. Laser calibration system using PULSE FFT Analyzer

Two examples of measurement are shown in Figure 8 and Figure 9.

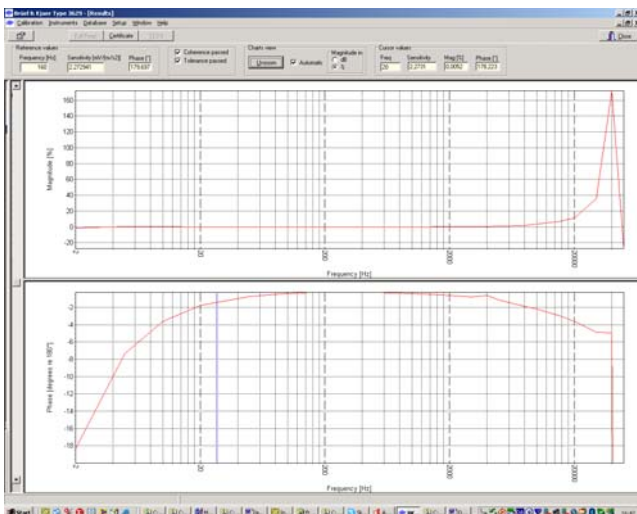


Figure 8. Wide range calibration of reference in shaker.

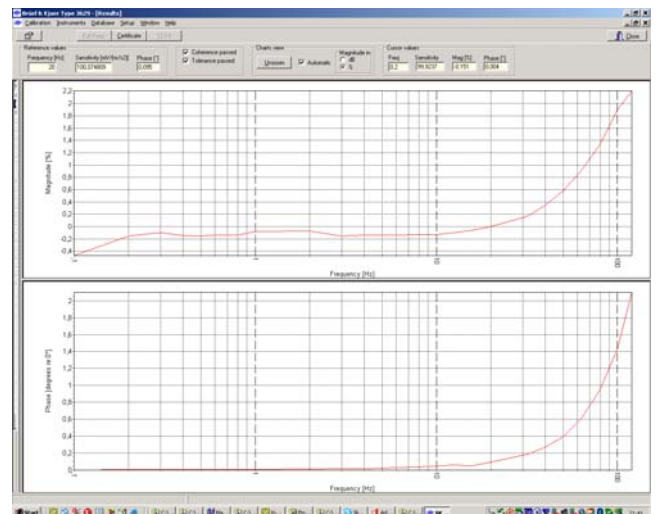


Figure 9. Calibration of servo accelerometer on long stroke shaker.

### 3.1 Problems and requirements

A problem for laser interferometry occurs at high frequencies, typically above 1 kHz. The calculation of the  $\varphi_{\text{Mod}}(t_i)$  values can graphically be explained as shown in Figure 10. Ideally the two laser detector outputs describe a circle if plotted on each of two perpendicular axes. However in practice two requirements have to be fulfilled before calculations can be made.

The first requirement is that the circle is not degenerated into an ellipse, corresponding to different sensitivities or intensities in the two channels. This can be corrected by normalizing the two signals.

The next requirement is that a center can be determined for the circle. When the displacement in the motion becomes less than about half a wavelength a full circle is no longer described and the center becomes increasingly difficult to find, resulting in increasing uncertainties.

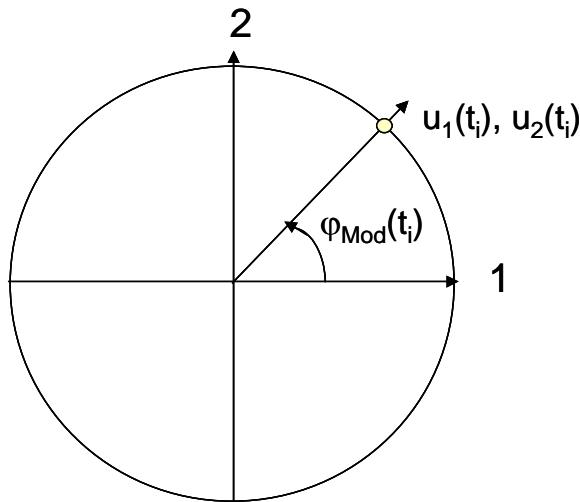


Figure 10. Determination of the Mod angle

This is avoided using the dual tone feature of the analyzer. By adding a suitable signal at a low frequency, typically in the 100 to 200 Hz range, a full circle is formed, and the high frequency motion is now a kind of modulation on top of the smooth motion of the point on the circle. When the analysis is performed afterwards it only means that we can find a signal at this frequency far away from the frequency of interest, which does not interfere with the measurement.

### 3.1 Evaluation of influences

Due to the modularity of the system it is possible to test the influence of different parameters on the data treatment and analysis. Raw data can be generated and stored just as the data from the PULSE front-end were stored. Then the system can use these data and give its results just as for normal calibrations. An example of a result is shown in Figure 9. The raw data are generated by means of a mathematical model in Mathcad containing both the fundamental calculus and noise on detectors and accelerometer and an ellipticity between the two channels.

Figure 12 and Figure 13 shows results from tests with ellipticity of 1 and 0.8. It is seen that the magnitude variations over the frequency range 0,3 to 3000 Hz is less than 0.05%, less than 0.1% to 10 kHz and remains below 0.6% up to 50 kHz. The phase deviations remain below 0,01 degree over the full frequency range as shown in Figure 13.

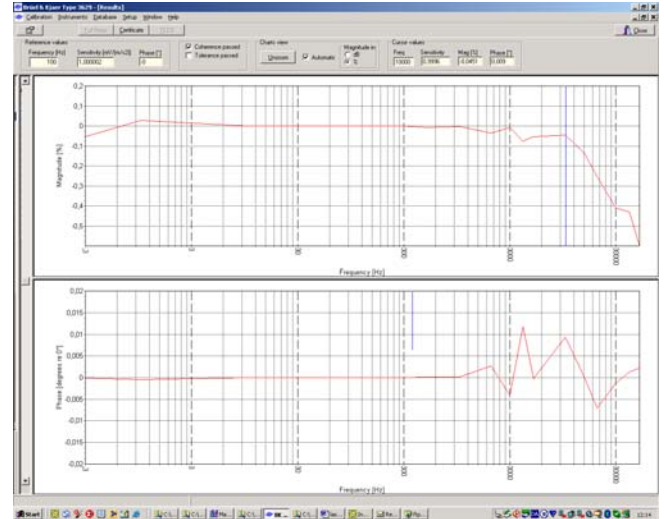


Figure 11. Result of simulation with 0.8 Ellipticity, as shown in the application.

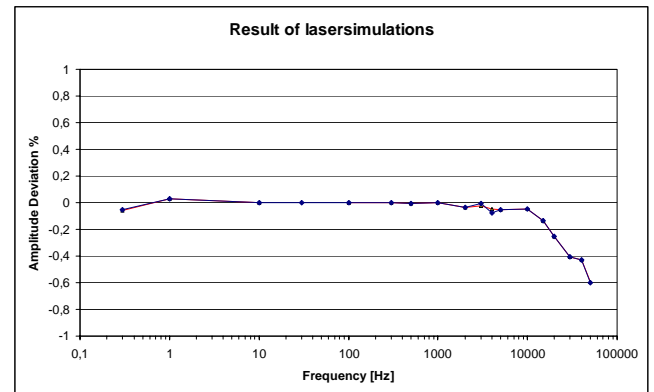


Figure 12. Amplitude Deviation Result of simulation with Ellipticity 0.8 and 1.

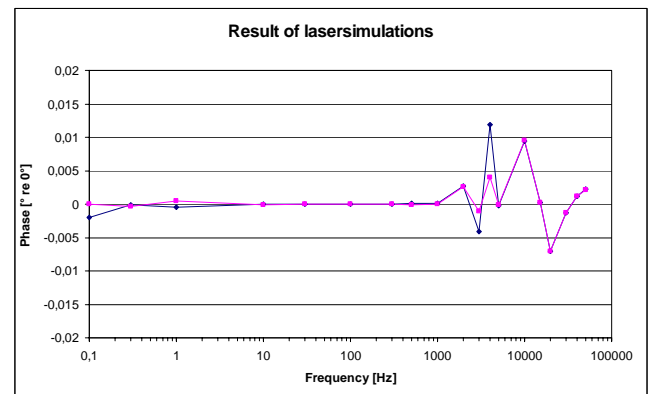
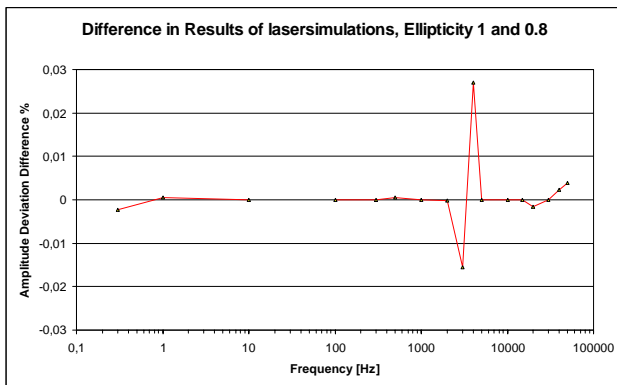


Figure 13. Phase deviation result of simulation with Ellipticity 0.8 and 1.

Figure 14 shows the difference in the obtained percentage variations on the magnitudes for ellipticity 0.8 and 1. The difference remains below 0.03% from 0.3 to 50000 Hz.



**Figure 14. Amplitude Deviation difference in percentage results of simulation with Ellipticity 0.8 and 1**

The calculated sensitivities at the reference frequency were all within  $\pm 0.0002$  % from the expected value.

#### 4. CONCLUSION

It has been proved that a system based on modern analyzers is well suited to perform primary calibrations following ISO 16063-11, Method 3.

The influence on the total measured sensitivity magnitude from typical noise and ellipticity variations has been shown to be less than 0.1% over the frequency range 0.3 Hz to 10 kHz and less than 0.6% up to 50 kHz.

The influence on the total measured sensitivity phase from typical noise and ellipticity variations has been shown to be less than  $0.001^\circ$  over the frequency range 0.3 Hz to 1 kHz and less than  $0.01^\circ$  up to 50 kHz.

#### REFERENCES

- [1] ISO 16063-11:1999. Methods for calibration of vibration and shock transducers - Part 11: Primary vibration calibration by laser interferometry. ISO 1999